TOR VERGATA
UNIVERSITÀ DEGLI STUDI DI ROMA

ACCADEMIA
NAZIONALE
DEI LINCEI

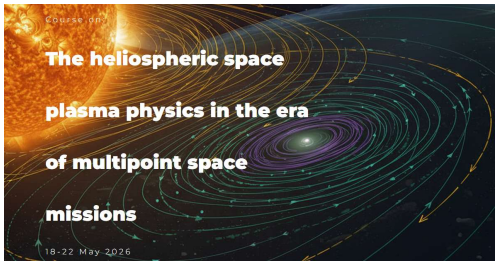

The active Sun: magnetic fields, flares, and surface organization

Francesco Berrilli (*francesco.berrilli@roma2.infn.it*)
1. Department of Physics – University of Rome Tor Vergata
2. Accademia Nazionale dei Lincei

TOR VERGATA
UNIVERSITÀ DEGLI STUDI DI ROMA

Outline

1. The changing magnetic Sun (Solar dynamos)
2. How Magnetic Fields Are Organized (magneto-convection)
3. Example 1: A Topological Algorithm for Solar Flare Forecasting
4. Example 2: Magnetic Imbalance and Scale Organization in Coronal Holes

TOR VERGATA
UNIVERSITÀ DEGLI STUDI DI ROMA

The Imperfect Sun: A Portrait of Dark and Bright Patches

In his 1613 work “History and Demonstrations Concerning Sunspots and Their Phenomena” Galileo Galilei used the term "clearer small squares" or "brighter patches" to describe what modern astronomers call solar *faculae*.


ISTORIA
E DIMOSTRAZIONI
INTORNO ALLE MACCHIE SOLARI
E LORO ACCIDENTI
COMPRESE IN TRE LETTERE SCRITTE
ALL'ILLVSTRISSIMO SIGNOR
MARCO VELSERI LINCEO
DELL'AVGVSTA
DAL SIGNOR
GALILEO GALILEI LINCEO
IN ROMA, Appresso Giacomo Mascardi. MDCXIII.
CON LICENZA DE' SVPERIORI.

TOR VERGATA
UNIVERSITÀ DEGLI STUDI DI ROMA

The Battle for Solar Luminosity: Sunspots vs. Faculae

Immediately after Galileo published his booklet on sunspot origins, his contemporary, *Giovan Battista Baliani*, raised two pioneering questions:

1. Do sunspots and faculae modulate solar brightness?
2. And do they influence the Earth?

Giovan Battista Baliani (1582-1666)

*As these **spots** clearly **block solar rays** (impediscono i raggi solari) , It's reasonable to believe these spots **could lead to changes in solar heat received (greater or lesser), regardless of seasonal or geographical areas**.*
*I would also respectfully request that Your Excellency extend the same degree of **scrutiny to the 'clearer small squares'** as has been applied to the sunspots, and hope that this may be addressed in future discourse.*

Genoa, 31 January 1614, Letter from Baliani to Galileo

TOR VERGATA
UNIVERSITÀ DEGLI STUDI DI ROMA

The Magnetic Origin of Sunspots and Faculae

ON THE PROBABLE EXISTENCE OF A MAGNETIC FIELD IN SUN-SPOTS.

By George E. Hale.

[Author's Abstract.[1]]

The lines in the spectra of Sun-spots differ from those of the ordinary solar spectrum mainly through changes of intensity and width. Most of the spot lines are more or less widened, some of them are double, and a few are triple. These characteristics of the lines, and the fact that the revolution of electrically charged particles in a solar vortex might be expected to produce a magnetic field, led to a search for evidences of the Zeeman effect in Sun-spot spectra.

Light from a spot was passed through a Fresnel rhomb and Nicol prism, mounted before the slit of a spectrograph of 30 feet focal length, used in conjunction with the tower telescope of the Mount Wilson Solar Observatory. Photographs of the spectra were made in the third order of a Rowland grating, having 14438 lines to the inch. It was found that the relative intensities of the components of the double lines in the spot are reversed by rotating the Nicol through an angle of 90°. The widened lines are also shifted when the Nicol is rotated. Just such changes are observed if the same doublets are examined under the same conditions along the lines of force of a powerful magnetic field.

When the Nicol is set at such an angle as to transmit the violet component and cut off the red component of a doublet in the spectrum of a spot surrounded by a right-handed vortex,[2] it will transmit the red component and cut off the violet component in the spectrum of a spot surrounded by a left-handed vortex. In the laboratory the same effect is produced by reversing the current in the magnet when observing the doublets along the lines of force. Hence the direction of revolution of the electrified particles in the vortex appears to determine the polarity of the resulting magnetic field, as theory requires. The observed polarity indicates that the Sun-spot field is produced by the motion of negative corpuscles.

[1] The article has since appeared in full in the November, 1908, issue of *Astrophysical Journal*.—Ed.

[2] The character of these vortices is shown on monochromatic images of the Sun made with the spectroheliograph, using the $H\alpha$ line of hydrogen.

159

160 G. E. HALE [Vol. XIII, No. 4]

The above results are obtained when the spots are near the center of the Sun. As they advance toward the limb, it might be expected that the doublets would change to triplets as is usually the case with doublets observed in the magnetic field. As this does not occur, it is of interest to note that all of the spot doublets hitherto observed in the laboratory (with one exception) have been found by Dr. King to appear as doublets not only when observed parallel to the lines of force, but also at right angles to the lines of force. As a matter of fact, a polariscopic study of these lines, made by Dr. King, shows that they are in reality quadruplets, though the components of each of the apparent doublets are so close together that they can not be separated in the Sun-spot spectrum. The line λ 6302.71, when observed at right angles to the lines of force in the laboratory, is an asymmetrical triplet, with the middle component displaced toward the red. In the spot spectrum it also appears as an asymmetrical triplet, with the middle component displaced toward the red. As some other lines also appear as triplets in the spot spectrum, it is evident that the light of the spot is partly longitudinal and partly transverse. A comparison of the separations of spot doublets with those of the same doublets observed in the laboratory gives, in the case of iron, a remarkably close agreement for the relative separations. In the case of titanium, and other elements extending through a considerable range of level in the Sun, there are greater divergences, probably due to the rapid change in the strength of the field in passing upward through the spot. The *D* and *b* lines in the spot spectrum, which represent comparatively high levels, show but little evidence of the magnetic field. Hence at the distance of the Earth the spot field would be quite inappreciable, even with very delicate instruments. The strength of the field in spots, at the level represented by the iron doublets, is about 2900 C. G. S. units.

The investigation is being continued, both on the solar and laboratory sides, and it is hoped that further results will soon be available.

Mount Wilson Solar Observatory.

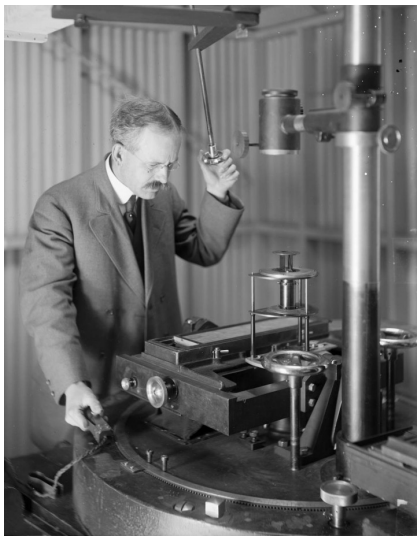

George Ellery Hale in 1908 discovered that sunspots are associated with strong magnetic fields.

5

TOR VERGATA
UNIVERSITÀ DEGLI STUDI DI ROMA

How Magnetic Fields Are Organized

TOR VERGATA
UNIVERSITÀ DEGLI STUDI DI ROMA

Core Architecture of the Solar Magnetic Field

1. **Spatial Scales & Regions**
   1. **Global Scale** (Magnetic Dipole): Dominates during solar minimum.
   2. **Local Scale** (Flux Tubes): Intense, compact magnetic structures found in sunspots (1-3 kG).
   3. **Active Regions** (Bipolar Groups): Clusters of sunspots with specific orientations that reverse polarity every 11 years.
2. **Field Configurations**
   1. **Closed Loops**: Anchor back into the surface; trap solar plasma.
   2. **Open Lines**: Extend into interplanetary space; drive the solar wind.

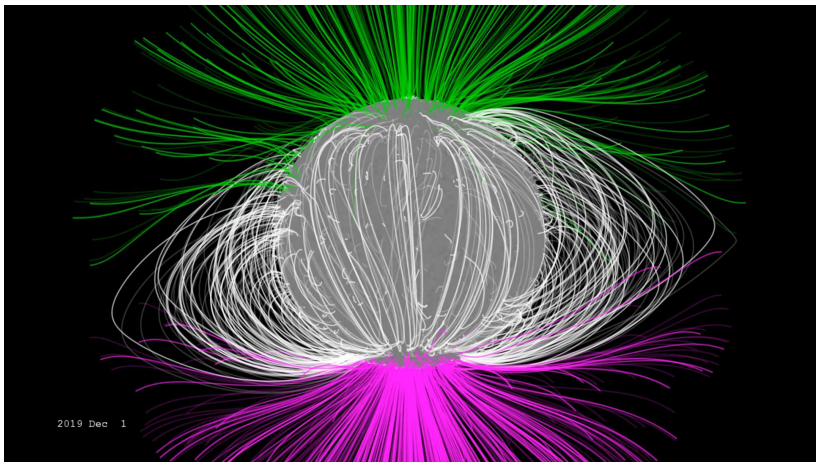

Solar magnetic field view from a fixed solar longitude with field lines using the conventional color scheme of green representing the positive (North) field and magenta as the negative (South) field. White field lines connect back to the solar photosphere.
Credits https://svs.gsfc.nasa.gov/5543/

7

TOR VERGATA
UNIVERSITÀ DEGLI STUDI DI ROMA

The Sun's total radiative output: Spots and Faculae and …..

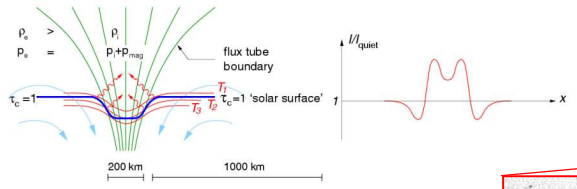

Sketch of a magnetic flux sheet (left) with corresponding intensity contrast (right) Steiner, 2007.

Different magnetic features contribute differently to solar irradiance variability

- The ratio between the size and the horizontal optical depth determine whether a structure is bright or dark.
- Brightness also depends on wavelengths and orientation (μ)

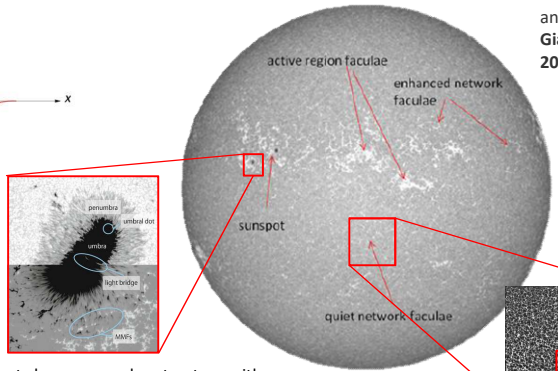

Sunspots have a complex structure with features like **umbra** and **penumbra**, and their appearance and contrast vary with their physical properties and location on the Sun's disk.
Kubo, in First Ten Years of Hinode Solar On-Orbit Observatory, (2018)

Magnetogram of a SG cell and intranetwork
Giannattasio+, A&A, 611, 2018

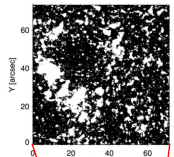

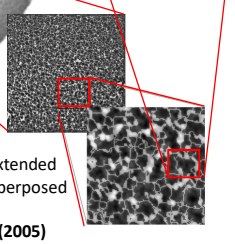

The *i-MAT* connected and extended **network** (white pixels) is superposed on the solar CAII K image.
Berrilli+, Sol. Phys. 228, 81 (2005)

8

TOR VERGATA
UNIVERSITÀ DEGLI STUDI DI ROMA

The Quiet Sun

Once thought to be entirely non-magnetic, the quiet Sun actually harbors a vast, hidden magnetic landscape driven by advection.

Polarized imaging reveals that these massive convective cells, spanning 1-30 Mm with lifetimes of few minutes (G) to 1 to 2 days (SG), use horizontal flows of several hundred m/s to clear out a myriad of weak intergranular/internetwork fields, organizing them into a reticular pattern of intense kilogauss fields known as the magnetic network (for SG).

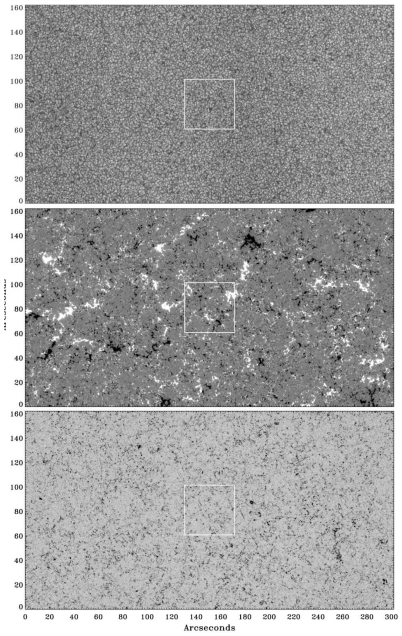

9

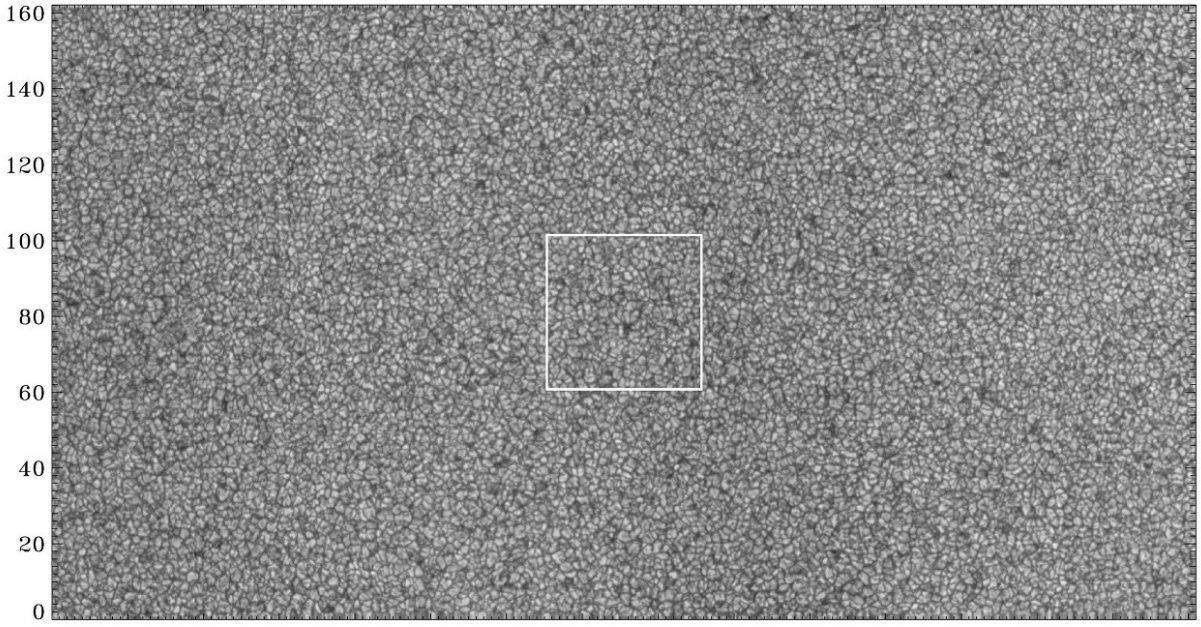

Quiet Sun at disk center as observed by the Hinode spectropolarimeter on 10 March 2007 between 11:37 and 14:37 UT. The panel shows a **continuum intensity map at 630 nm**. Images reproduced with permission from Lites et al. (2008), copyright by AAS

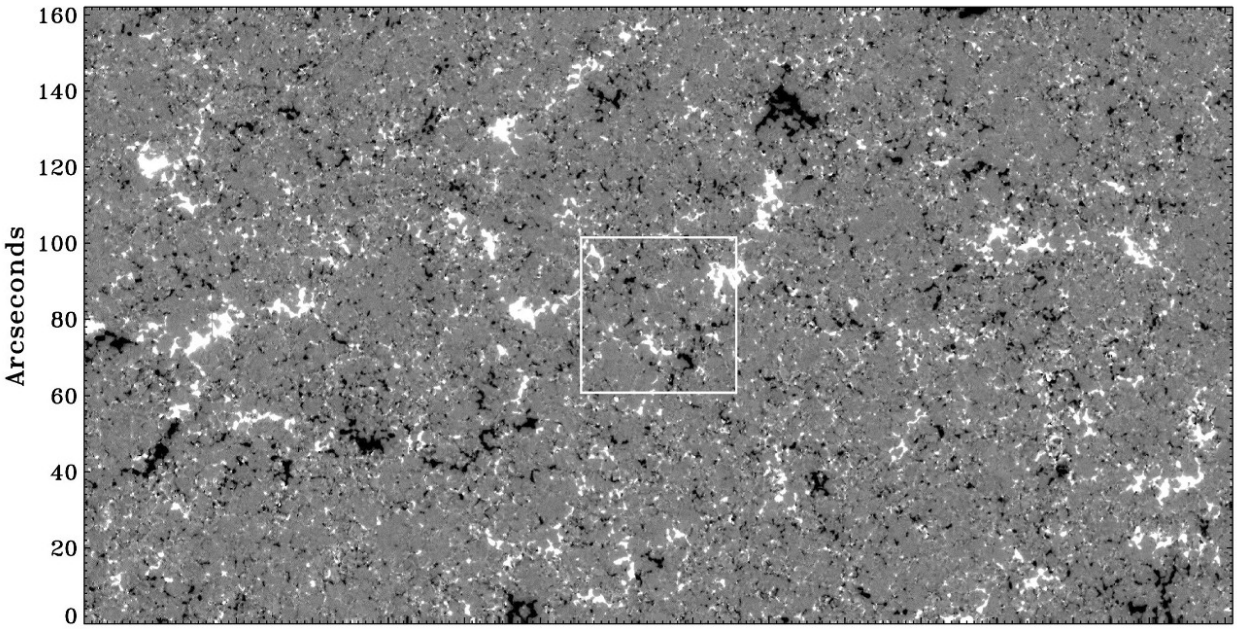

Quiet Sun at disk center as observed by the Hinode spectropolarimeter on 10 March 2007 between 11:37 and 14:37 UT. The panel shows the corresponding maps **of longitudinal magnetic flux density derived from the circular polarization signals observed in the Fe I 630 nm line pair**. The gray scales saturate at ±50±50 Mx cm−2−2 and 200 Mx cm−2−2, respectively. Images reproduced with permission from Lites et al. (2008), copyright by AAS

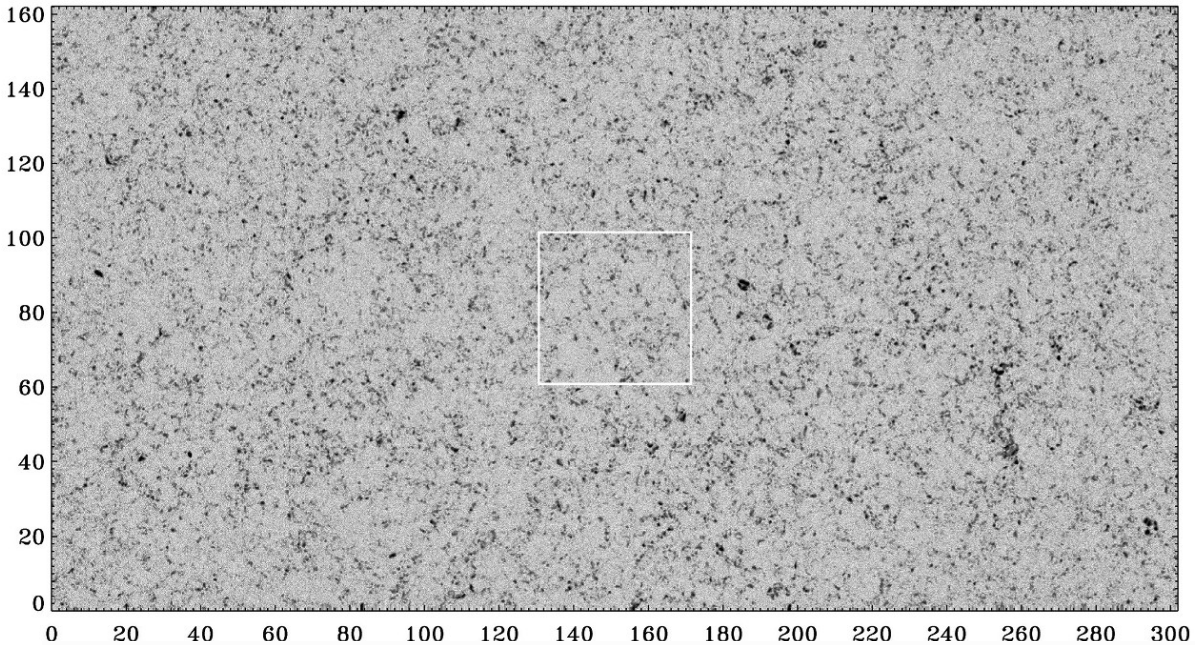

Quiet Sun at disk center as observed by the Hinode spectropolarimeter on 10 March 2007 between 11:37 and 14:37 UT. The panel shows the corresponding maps **transverse flux density** derived from the **linear polarization signals observed in the Fe I 630 nm line pair**. The gray scales saturate at ±50±50 Mx cm−2−2 and 200 Mx cm−2−2, respectively. Images reproduced with permission from Lites et al. (2008), copyright by AAS

Plasma Evacuation & Buoyancy

Radial force balance across the flux tube boundary creates a significant pressure differential:

- **Strong Evacuation**: Magnetic pressure necessitates a reduction in internal gas pressure:

$$p + \frac{B^2}{8\pi} = p_e$$

  where p_e and p_i are the external and internal gas pressure, respectively, and $B^2/8\pi$ is the magnetic pressure for a field strength B.
- **Density Deficit**: Evacuation leads to considerable magnetic buoyancy

$$\rho_e - \rho_i = \frac{B^2}{2\mu_0 RT} \quad (> 0)$$

- **Vertical Alignment**: Buoyancy forces ensure magnetic fields remain nearly vertical on average.

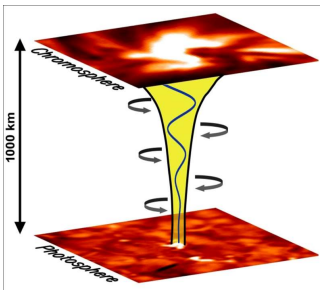

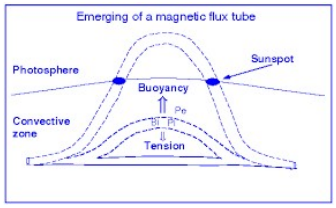

Credits: Axel Brandenburg

Flux Transport Dynamics

The interaction between plasma and magnetic field governs the distribution of flux on the solar surface.

- **Flux Freezing:** Large magnetic Reynolds numbers ($R_m = UL/\eta \gg 1$) bind field lines to fluid elements.
- **Network Formation:** Horizontal convective flows transport flux to down-draft regions.
- **Induction Dominance:** Bulk motions redistribute magnetic flux until local energy ratios favor the field.

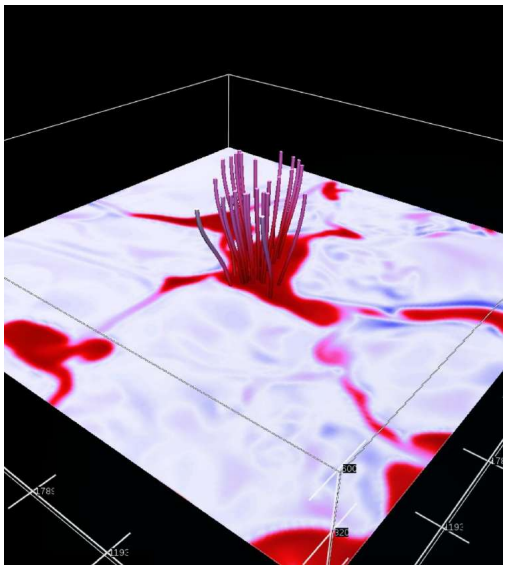

TOR VERGATA
UNIVERSITÀ DEGLI STUDI DI ROMA

Organization of magnetic elements in the quiet Sun

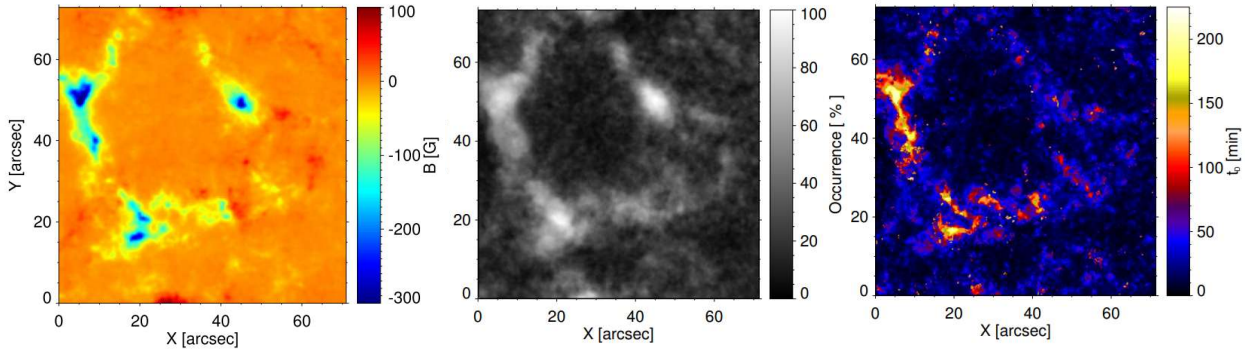

Fig. 1. Mean magnetogram of the FoV averaged over ~24 h, the whc
time range of the series.

Highly recurrent and persistent patterns were detected especially in the boundary of the supergranular cell. These are due to moving magnetic elements undergoing motion that behaves like a random walk together with longer decorrelations (~2 h) with respect to regions inside the supergranule. Giannattasio+, 2018

15

TOR VERGATA
UNIVERSITÀ DEGLI STUDI DI ROMA

Organization of magnetic elements in the quiet Sun

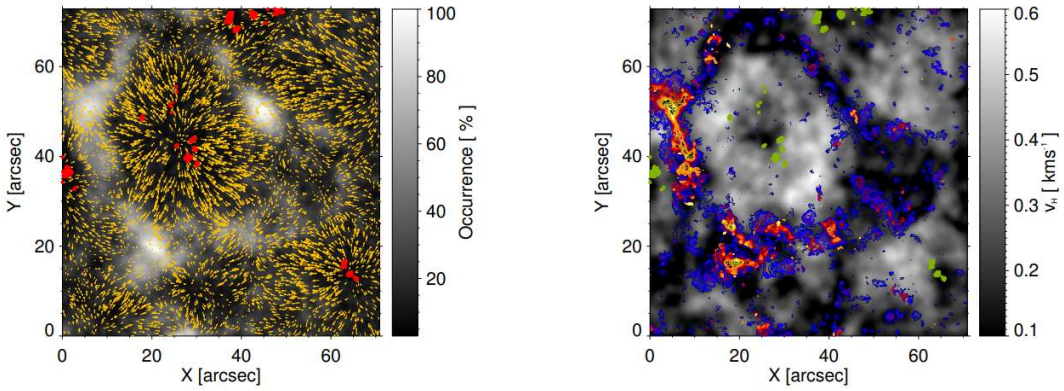

Left: horizontal velocity field (gold arrows) computed with FLCT (Fisher & Welsch 2008) superimposed to the occurrence map. The **red filled circles mark the locations with the lowest occurrences** (≤ 5%). Right: Horizontal velocity strength map (grey scale). The decorrelation times map for t_D > 20 min is superimposed. The **green filled circles mark the locations with the lowest occurrences** (<5%). Giannattasio+, 2018

16

TOR VERGATA
UNIVERSITÀ DEGLI STUDI DI ROMA

From the quiet sun to the active regions

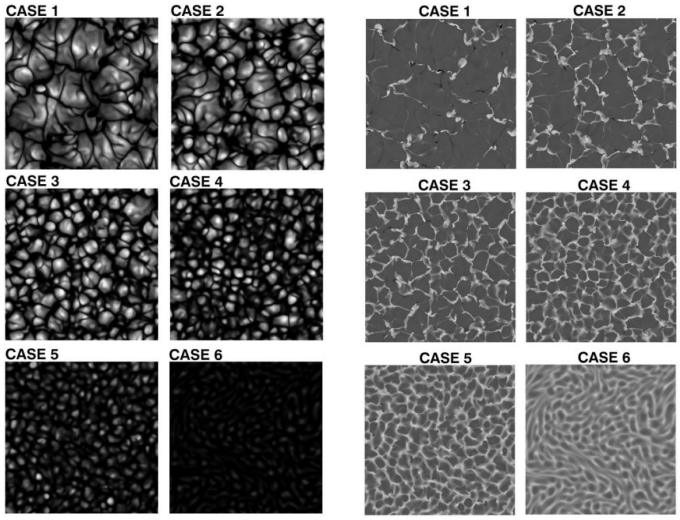

Cattaneo, Emonet, Weiss, On the interaction between convection and magnetic fields, ApJ, 588:1183–1198, 2003

Left: Snapshots showing temperature fluctuations near the upper surface for cases 1–6. The scaling is the same for each case. **As B_0 is increased, the cells grow narrower and convection becomes feebler, so that the range of variation in the temperature diminishes**
Right: Surface magnetic field. In these gray-scale plots dark and light regions again denote oppositely directed fields, and the scaling is the same for all cases. Note that fields with both directions are present in case 1, but the imposed field direction predominates as B_0 is increased. **The mesocellular pattern persists in the convective regime (cases 1 and 2), but only smaller cells are present in the intermediate regime.**

17

TOR VERGATA
UNIVERSITÀ DEGLI STUDI DI ROMA

From the quiet sun to the active regions

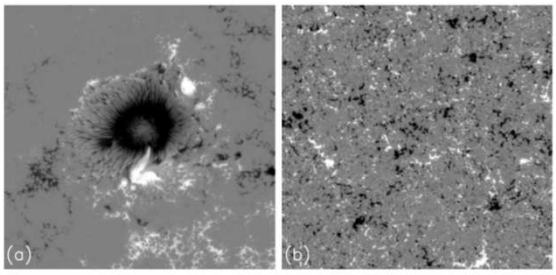

Figure 1: Stokes V in blue wing of 630.2 nm line from Hinode. Around a sunspot (a) and in the quiet Sun (b), showing the wide range in size of magnetic structures on the Sun. The dimensions of both figures are 110 Mm and the pixel size is 108 km. Image reproduced by permission from Parnell *et al.* (2009), copyright by AAS.

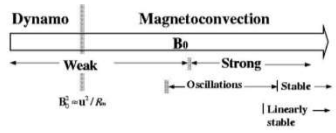

FIG. 4.—Schematic representation of the different regimes obtained as the value of the net magnetic flux through the box is increased. Thick solid lines denote hard transitions, while fuzzy lines indicate more gradual transitions.

The solar surface is covered with magnetic features with spatial scales from smaller than can currently be resolved to active regions covering up to 100 Mm. These evolve on a correspondingly wide range of time scales, from seconds for the smallest observed features, to months for some active regions.

R. Stein, *Solar Surface Magneto-Convection*, Living Rev. Solar Phys., 9, 2012

On the extreme left are cases in which the imposed field is zero and on the extreme right, cases in which the imposed field is strong enough to suppress convection altogether.

Cattaneo, Emonet, Weiss, On the interaction between convection and magnetic fields, ApJ, 588:1183–1198, 2003

18

TOR VERGATA
UNIVERSITÀ DEGLI STUDI DI ROMA

Example 1: A Topological Algorithm for Solar Flare Forecasting

Cicogna D., Berrilli F., Calchetti D. and 6 more, *Flare-forecasting Algorithms Based on High-gradient Polarity Inversion Lines in Active Regions*, The Astrophysical Journal, 915, id.38, 2021

We present a scientific case in which the **topology** of the magneto-convective structures have an effect on solar phenomena:

Probability of flare (D value algorithm)

In other words, can the topology of an active region help us predict the onset of a flare?

D VALUE ALGORITHM

Cicogna, D., Berrilli, F., Calchetti D., Del Moro D., Giovannelli L., Benvenuto F., Campi C., Guastavino S. & Piana M., *Flare-forecasting Algorithms Based on High-gradient Polarity Inversion Lines in Active Regions*, ApJ, 915, id.38, 2021

D is a topological parameter based on the automatic recognition of magnetic **polarity inversion lines (PILs)** in ARs capable of estimating their complexity.

We use a ML method to validate the effectiveness of the descriptor to predict the occurrence of X- or M-class flares during the following 24 hr period.

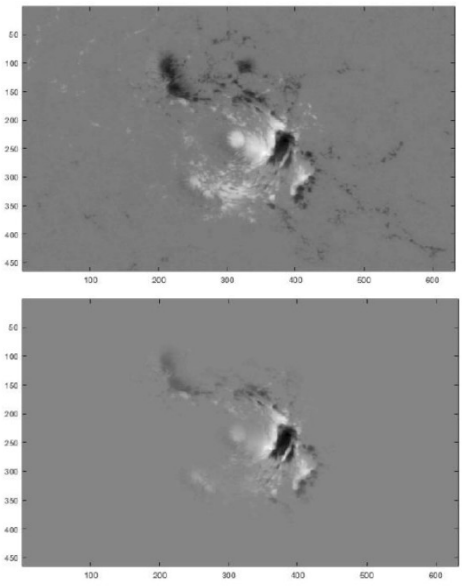

Upper: SDO HMI magnetogram of AR 12673 (NOAA number) on 5 September 2017, with an X9.3 are within 24hours. Lower: HMI magnetogram multiplied for the weighting map. The summation over all pixels gives R. The number of PILs gives D.

Let‘s take the example of three objects (**glass**, **cup** and **teapot**) that are used for the same purpose, i.e., to contain liquid
空 /kòng/ empty, void

We can insert the same amount of liquid (analogously to the same amount of magnetic energy) but the topological properties are different.

In practice, the shape (**morphology**) allows them to contain the same quantity of liquid (or magnetic energy) but the possibility of different uses (complexity) changes as the **topology** changes.

We apply to the **SDO/HMI photospheric magnetogram** an absolute thresholding technique to prepare three different bitmap images: I_+, I_-, and I_U.

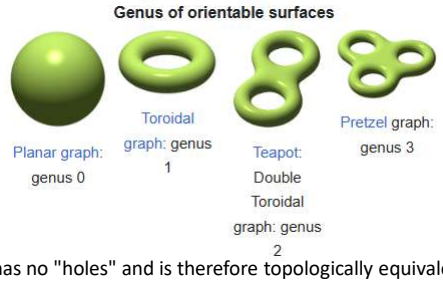

The **glass** has no "holes" and is therefore topologically equivalent to a sphere (genus 0), the **cup** has a "hole=handle" and is equivalent to a donut (genus 1), a **teapot** has two "holes=handle+spout" and is equivalent to a two-holed donut (genus 2).

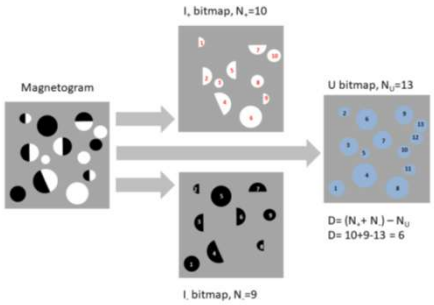

Figure 3. The scheme for calculating the D value consists of few simple steps. First, a segmentation and labeling technique applied to the magnetogram identifies and counts the number of compact flux density structures in the three bitmaps, N_+, N_-, and N_U, respectively. Successively, the difference $D = (N_+ + N_-) - N_U$ counts the number of PIL fragments in the magnetogram.

- We selected LOS magnetograms within 45 degrees from disk center for each day from June 2010 to June 2018.
- We compared the magnetogram dataset with the GOES flare list to label magnetograms as flaring or non-flaring.
- The analyzed set is composed of 100 magnetograms of different HARPs hosting an M- or X-class are in the next 24 hours.
- The non-flaring set is composed by a collection of HARPs that did not produce any M- or X-class flare during their lifetime. This control group includes 745 total magnetograms.

Class	D = 0 (%)	D = 1 — 2 (%)	D = 3 — 6 (%)	D = 7 — 9 (%)	D ≥ 10 (%)
>M1	2	13	26	80	96
>X1	0	∼ 0	1	4	26

Likelihood of M or X are within 24 hours from the determination of the D parameter, similarly to Tab.1 in Schrijver (2007).

Out of nearly 200 tested predictors, D is uniquely consistent. It is the only parameter that achieves a top-ten ranking across all testing scenarios used to compute predictor weights for solar flare forecasting.

This result is a quantitative confirmation of the correlation between AR complexity and the probability of flare emission.

Please refer to the paper Cicogna +, 2021 for more details.

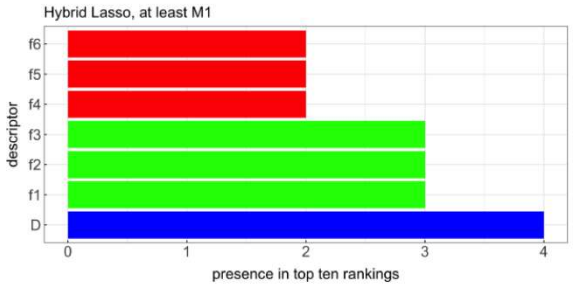

Figure 7. Histograms counting the number of times predictors are in the top-10 rankings, on average over the 100 random realizations of the training and test sets. Descriptors from "f1" to "f6" are "sfunction_blos/zq", "sharp_kw/snetjzpp/total", "sharp_kw/ushz/stddev", "decay_index_br/maxl_over_hmin", "helicity_energy_bvec/abs_tot_dedt_in", "wlsg_br/value_int", respectively, and their description can be found in Table 6.

Descriptor	Definition
"wlsg_blos/value_int" and "wlsg_br/value_int"	B_{los} and B_{radial} Falconer's $^{L}WL_{SG}$
"mpil_blos/tot_length"	Total length of all MPILs
"mpil_blos/max_length"	Maximum length of a single MPIL
"mpil_blos/tot_usflux"	Total unsigned flux around all MPILs
"sfunction_blos/zq"	tifractal structure function inertial range index
"sharp_kw/snetjzpp/total"	Sum of absolute value of net currents per polarity
"sharp_kw/ushz/stddev"	Standard deviation of the unsigned vertical current helicity
"decay_index_br/maxl_over_hmin"	Maximum ratio of MPIL length to minimum height of critical decay index
"helicity_energy_bvec/abs_tot_dedt_in"	Absolute value net vertical Poynting flux

Table 6. List and definitions of the mentioned descriptors from the FLARECAST project.

TOR VERGATA
UNIVERSITÀ DEGLI STUDI DI ROMA

Example 2: Magnetic Imbalance and Scale Organization in Coronal Holes

Cantoresi M., Berrilli F., Lepreti F., *Organization scale of photospheric magnetic imbalance in coronal holes*, Rendiconti Lincei. Scienze Fisiche e Naturali, Springer Nature, 34, 1045, 2023

Cantoresi M. & Berrilli F., *Magnetic Imbalance at Supergranular Scale: A Driving Mechanism for Coronal Hole Formation*, Solar Physics, 299, id.101, 2024

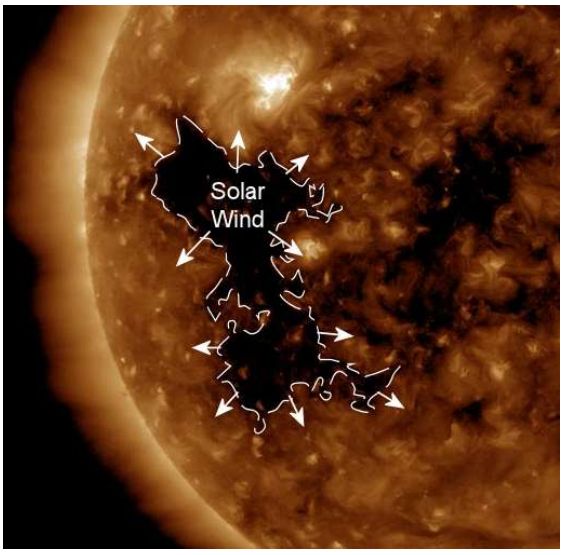

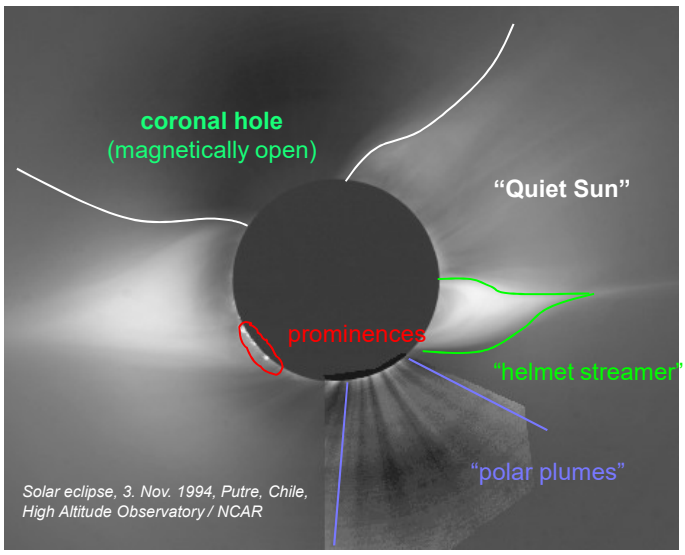

When a large-scale coronal hole emerges, it can launch a high-velocity, low-density stream of solar wind toward Earth. The interaction between this plasma stream and Earth's magnetosphere is expected to trigger a geomagnetic storm.

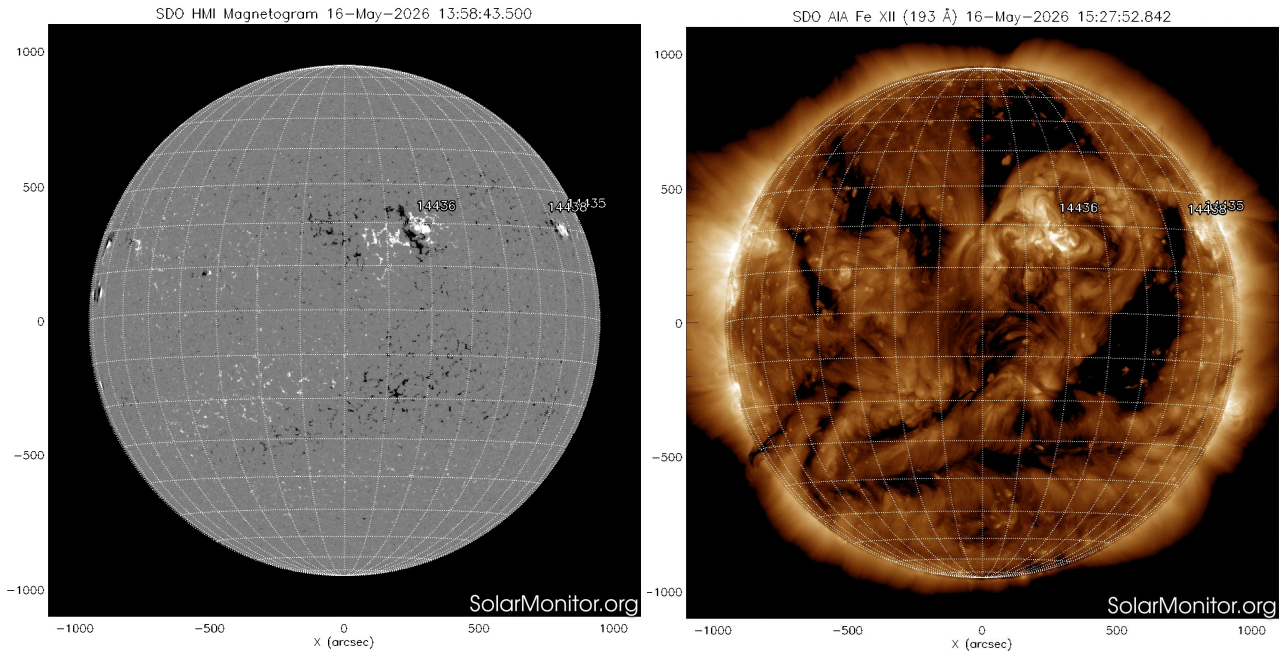

CHs are the source regions of the fast solar wind, coronal magnetic field lines are mainly open, and associated photospheric fields imbalanced in polarity

Still many open questions, such as:

1. How do they originate?
2. What is the cause of the magnetic field imbalance?
3. How is solar wind accelerated?

Coronal Holes: Photospheric characterization

In order to study the properties of the magnetic field associated with CHs we have:

downloaded series of magnetic field (SDO/HMI) and corona maps in the EUV (SDO/AIA);

Used numerical procedures for the segmentation of CHs in SDO/AIA coronal images

Selected Regions Not Associated to CHs (NCHs) as control group

Reprojected CH and NCH boundaries to HMI magnetograms and selected Regions of Interests (RoIs)

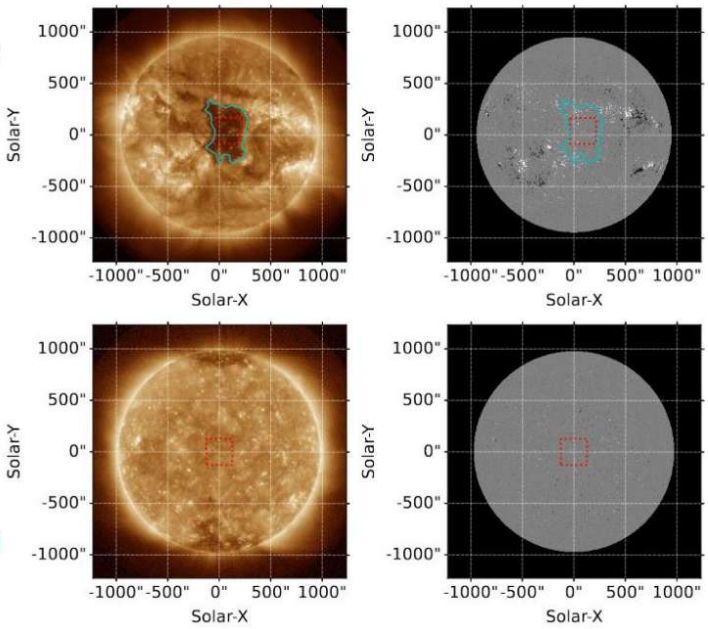

Coronal Holes: Analysis Scheme

To estimate the properties of the photospheric magnetograms underlying the different ROIs three types of analysis were performed:

1. The study of the standardized moments (e.g., *mean*, *skewness*) of the B_{LoS} distribution;

2. Cancellation analysis of the observed (and simulated) magnetograms underlying the ROIs;

3. Study of the diffusivity of magnetic elements of CHs

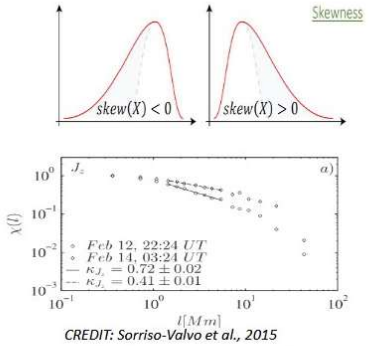

CREDIT: Sorriso-Valvo et al., 2015

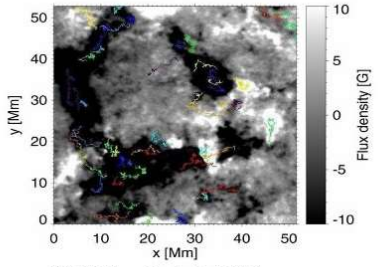

CREDIT: Giannattasio et al., 2013

Analysis of the Distributions of CHs and NCHs fields

The absolute value of the standardized moments of the B_{LoS} distributions for a statistic of 60 CHs and 60 NCHs is reported. The analysis of the standardized moments for CHs and NCHs shows the imbalance of B_{LoS} in the CHs magnetograms.

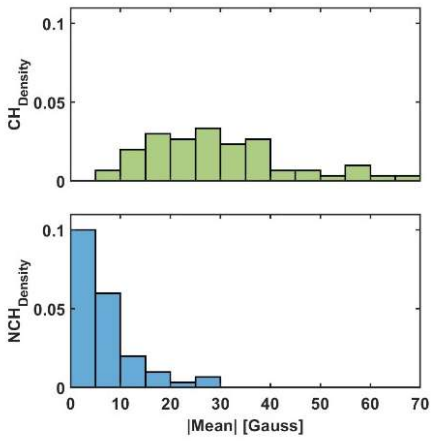

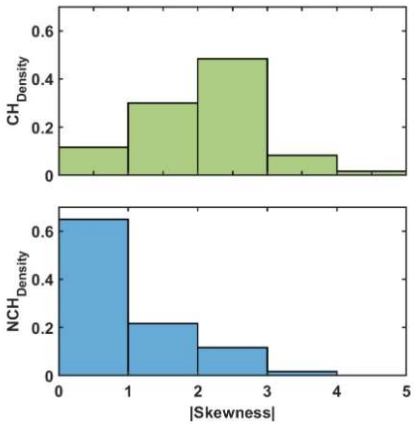

From Cantoresi et al., 2023

Cancellation Analysis

Consider a field *f(r)* and its domain *Q(L)*. Let be *Qi(l)⊂Q(L)* a partition of *Q(L)* in disjoint subsets of size *l*. The signed measure is:

$$\mu_i(l) = \frac{\int_{Q_i(l)} dr f(r)}{\int_{Q(L)} dr |f(r)|}$$

The cancellation function can be calculated as:

$$\chi(l) = \sum_{Q_i(l)} |\mu_i(l)|$$

For fields which satisfy the property of self similarity:

$$\chi(l) = l^{-k}$$

where **k is the cancellation exponent**.

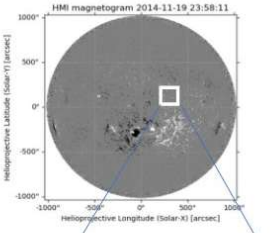

B11	B12	B13	B14
B21	B22	B23	B24
B31	B32	B33	B34
B41	B42	B43	B44

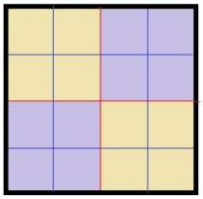

If a given field changes sign on arbitrarily small scale, it is called **sign singular** (*Sorriso-Valvo+ 2015*). k says how much the sign is singular:

- if *k=1* the sign of f is strongly singular. This case occurs if *f* is a Brownian noise
- If *k=0* the field f is smooth and the sign is not singular
- **Intermediate cases indicate the presence of smooth fields in random fluctuations**

Results: CH magnetic fields cancellation analysis

The Cancellation Analysis is performed on photospheric magnetograms associated with 60 CHs and 60 NCHs.

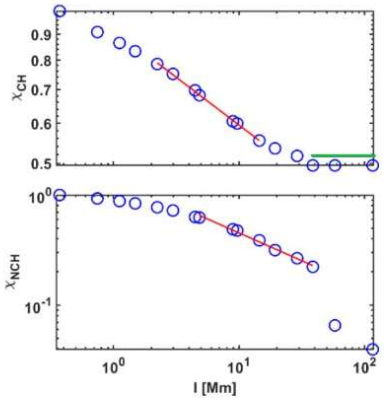

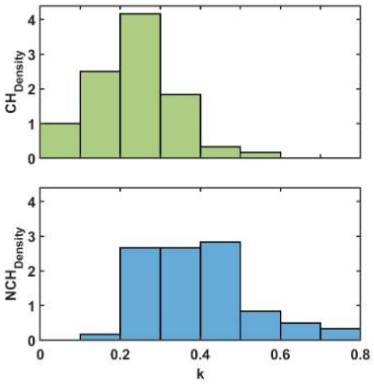

In more than 80% of the magnetograms associated with CHs, a plateau is observed starting at SG. Instead, less than 20% of the magnetograms associated with NCHs show the presence of a plateau

From Cantoresi et al., 2023

Photospheric Magnetic Pattern Simulation

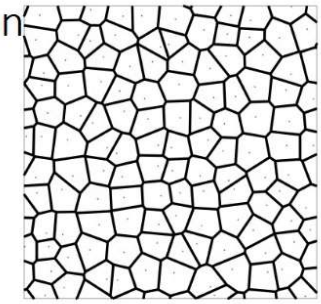

To interpret these results, we carried out numerical simulations that mimic photospheric magnetic patterns.

Two organizations of solar magnetic fields are considered:

1. weak ubiquitous bipolar fields populating the intranetwork regions, modelled with a Gaussian matrix;
2. magnetic elements accumulated at the SG boundaries, modelled considering magnetic concentrations in the boundaries of a Voronoi

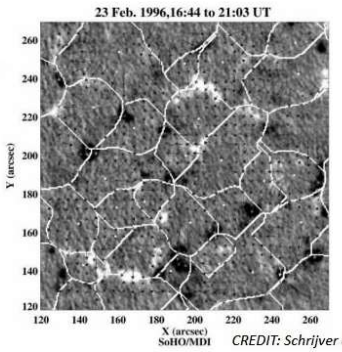

CREDIT: Schrijver et al., 2009

In simulated CHs magnetic elements have the same sign, in NCH it is random

Simulations VS Analysis Results

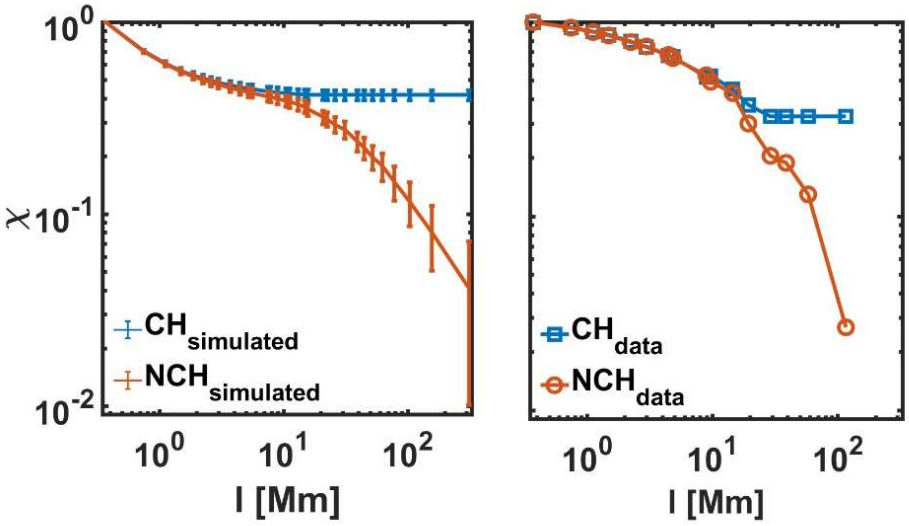

The difference between CH and NCH cancellation functions emerge mainly on larger scales, in both cases. Simulated reproduces correctly the plateau observed in χ_{CH} measured

The imbalance of Coronal Hole photospheric magnetic fields: distributions and cancellation analysis

In CHs higher values of mean and skewness are more probable

CHs magnetic fields are imbalanced

At larger scales the CH cancellation function is shallower than that of NCH. In CHs at the supergranular scale the sign is no more singular

Typically, the imbalance of B_{LoS} in the CHs magnetograms emerges at supergranular scales

Unipolar patches (funnel roots) are rooted in the network.

Magnetic pattern simulations

In agreement with the current literature (i.e. Hofmeister et al., 2017 and Bale et al., 2023)

Adapted from Cantoresi et al., 2023

Diffusivity of magnetic elements: extraction and tracking

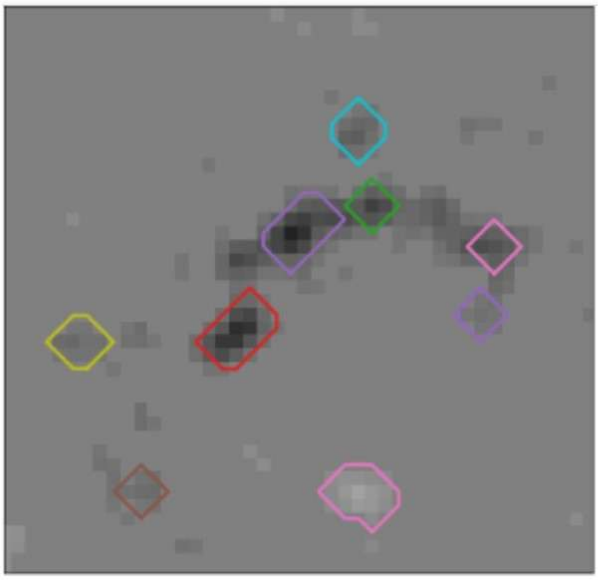

We studied the photospheric magnetic fields dynamics (48h) of 17 CHs.
The analysis scheme is the following:

1. Download of HMI magnetogram
2. Segmentation of MEs defined as the local maximum of the magnetic fields
3. Tracking the magnetic elements
4. Study of the displacement spectrum of the MEs with the dominant and non-dominant polarity

Anomalous Diffusion

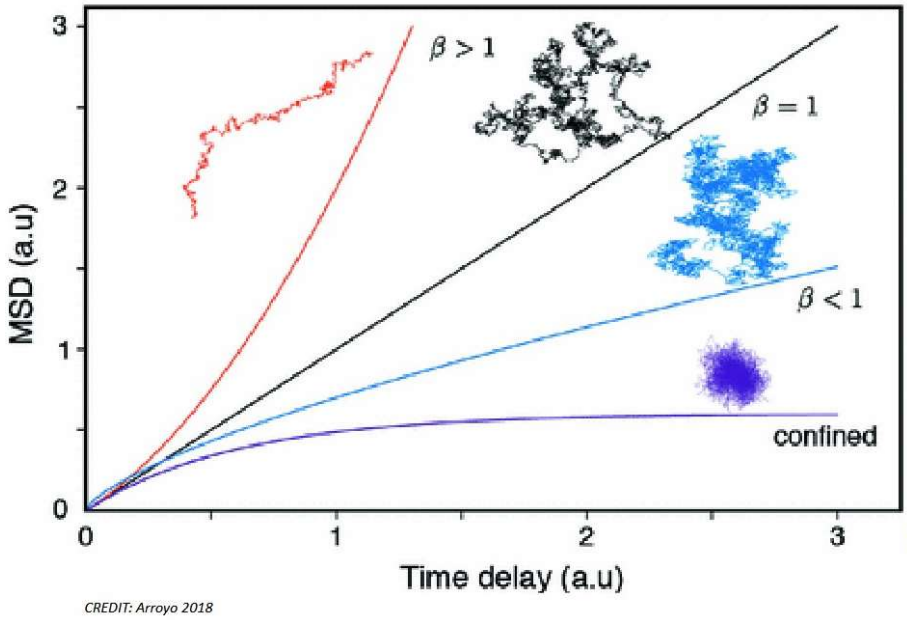

CREDIT: Arroyo 2018

Normal diffusion phenomena can be modelled through the scaling law

$$< r^2 > \sim \tau^{\gamma}$$

With γ=1

If γ ≠1 the diffusion is anomalous.

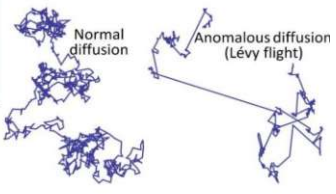

Analysis and Results

We studied the traces of 401978 m.e. with dominant and 221802 m.e. with non dominant polarity

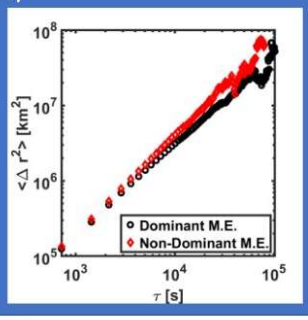

We performed a bootstrapping at the 35% of the m.e. We calculated the diffusion index for the two populations of m.e. by performing a linear fit, in log scale

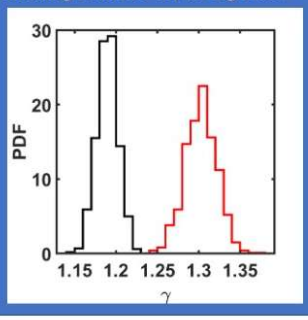

Dominant Polarity m.e. diffuse in a less efficient way. Consequently, they are associated to the supergranular network, confirming our previous hypothesis.

Main Points and Key Takeaways

- **Magnetic Field Architecture:** The Sun's magnetic structure operates across various scales. It transitions from a global-scale dipole configuration (prominent during solar minimum) to localized, high-intensity "flux tubes" (1–3 kG) within active regions. These regions form bipolar clusters that completely reverse polarity every 11 years, with plasma either trapped in closed loops or escaping along open lines.
- **Organization of the "Quiet Sun":** The quiet Sun contains a hidden network of weak magnetic fields organized by large convective cells (supergranulation). Horizontal plasma flows push these fields to the boundaries of the cells, forming an intense kilogauss magnetic network. Additionally, the drop in internal gas pressure within these fields creates a buoyancy force that keeps them standing nearly vertical.
- **Topological Forecasting (D-Value Algorithm):** Solar flare prediction relies heavily on structural complexity rather than just raw magnetic energy volume. Using machine learning to analyze line-of-sight magnetograms, researchers created a topological parameter (D) based on high-gradient polarity inversion lines. This parameter successfully ranked in the top ten out of nearly 200 tested predictors for forecasting M- or X-class flares within 24 hours.
- **Coronal Holes and Plasma Dynamics:** Coronal Holes (CHs) serve as the main source regions for the fast solar wind. They are characterized by magnetically open field lines and a net imbalance in magnetic polarity at the photospheric level. Significant questions remain regarding their exact origin, the cause of this polarity imbalance, and the precise mechanisms accelerating the wind.